

Original Research Paper

Dispersion Modeling of SO₂ and NO₂ Emissions Using AERMOD on Ambient Air Quality at Steam Power Plant PT.X in Southeast Sulawesi, Indonesia

Nur Miftahuljannah, Sumarni Hamid Aly[†] and Muralia Hustim

¹ Department of Environmental Engineering, Hasanuddin University, Malino Str. km 6, Gowa, South Sulawesi, 92171, Indonesia

[†] Corresponding author: Sumarni Hamid Aly; marni_hamidaly@yahoo.com

ORCID IDs of Authors: 0009-0007-2300-7810¹, 0000-0002-8328-1930^{1†}, 0000-0001-8323-1549¹

Key Words	AERMOD; Dispersion modelling; Model validation; Steam power plant industry; SO ₂ and NO ₂ Emissions; Ambient air quality
DOI	https://doi.org/10.46488/NEPT.2026.v25i03.D1894 (DOI will be active only after the final publication of the paper)
Citation for the Paper	Miftahuljannah, N., Aly, S. H., and Hustim, M., 2026. Dispersion modeling of SO ₂ and NO ₂ emissions using AERMOD on ambient air quality at steam power plant PT.X in southeast Sulawesi, Indonesia. <i>Nature Environment and Pollution Technology</i> , 25(4), D1894. https://doi.org/10.46488/NEPT.2026.v25i03.D1894

Abstract: This study aims to analyze SO₂ and NO₂ concentrations around the PT.X power plant through direct measurements, model their distribution patterns using AERMOD, and evaluate the model's performance using RMSE, MBE, and R statistical tests. Monitoring was conducted at two monitoring points (PLTU PT.X Area and Nii Tanasa Village) over four 1-hour intervals (morning, afternoon, evening, night) using an Impinger Air Sampler. The results show that the highest field-measured SO₂ (39.95 µg/m³) and NO₂ (14.82 µg/m³) occurred during the day, whereas AERMOD predicted peak concentrations at night, reaching SO₂ (31.87 µg/m³) and NO₂ (10.56 µg/m³) at the PLTU PT.X monitoring point, indicating stable atmospheric conditions. Pollutant distribution aligns with the prevailing north-northeast winds, with concentrations decreasing significantly by distance and remaining within regulatory limits. Statistical validation for SO₂ and NO₂ yielded RMSE values of 14 µg/m³ and 5.37 µg/m³, MBE of -10.44 µg/m³ and -4.32 µg/m³, and R of 0.36 and 0.12, respectively. These values reflect the inherent challenges of aligning short-term field data with long-term dispersion modeling. It is concluded that spatial proximity to emission sources is the primary factor determining concentration patterns. While acknowledging temporal limitations for full-scale validation, the AERMOD model serves as a valuable preliminary screening tool for these distribution patterns. These findings provide an initial overview to inform decision making and support the development of effective emission mitigation and environmental management strategies for the surrounding areas.

1. INTRODUCTION

Steam Power Plants (PLTU) serve as a vital energy source for industrial activities (Munawaroh et al., 2019). The primary fuel utilized in the power plant industry is coal (Octaviani et al., 2023). According to Rahmadina (2022), this reliance stems from the abundant supply of coal, which is utilized as a major electricity source for various industries, particularly steam power generation.

PLTU PT.X is one such power plant located in Lalonggasumeeto District, Konawe Regency, Southeast Sulawesi was established in 2007 and has been in commercial operations since 2013, utilizing low-calorie lignite coal for power generation (Barata, 2024). In its operations, the activities of PLTU PT.X which also utilize coal have the potential to emit gaseous pollutants such as Sulfur Dioxide (SO₂) and Nitrogen Dioxide (NO₂). It is critical to monitor these emissions as they disperse into the surrounding air and pose potential risks to local public health (Ningsih, 2020). According to Tampa et al. (2020), SO₂ exposure can lead to respiratory tract irritation and decreased pulmonary function; similarly, NO₂ can cause mucous membrane irritation and potentially lead to pulmonary edema in cases of high-dose, long-term exposure, acting as a primary trigger for respiratory diseases (Alchamdani, 2019). This health risk is evidenced by the increase in cases of acute respiratory infection reported at the Lalonggasumeeto Public Health Center from 2015 to 2020 (Halulanga et al. 2021).

In anticipating the potential negative impacts of PLTU PT. X activities, gas-emission distribution modeling is needed as an initial mitigation step to analyse air quality relative to pollutant distribution, establish relationships between emitted pollutants and their concentrations, and identify affected areas (Wangsa et al. 2022). Various models commonly used in predicting air pollutant dispersion include HYSPLIT, CALINE-4, AERMOD, CALPUFF, WRFChem, and GRAL (Alviani et al. 2022). This study uses AERMOD to model emission dispersion. This model is recommended by the United States Environmental Protection Agency (US EPA) because it has been proven effective in analyzing, predicting, and simulating the distribution of SO₂ and NO₂ emissions (Zakaria et al. 2020), taking into account meteorological and topographic factors (Putra & Nisa, 2023), and can estimate the air quality impact of up to 50 different sources, whose configurations include points, areas, and volumes (Nugraha et al. 2023). Widely recognized as a leading Gaussian plume model, AERMOD is utilized to estimate the environmental consequences resulting from multiple air pollution sources (Salari et al. 2026). This method has also been widely applied internationally to predict pollutant concentrations from various industrial point sources. For example, a study in Cam Pha, Vietnam, showed that AERMOD was successfully applied to evaluate the impact of power plant emissions, involving model validation with observational data (Tran et al. 2022). Similarly, in Indonesia, AERMOD has been used to predict SO₂ and NO₂ dispersion at the PLTU PT. Semen Tonasa uses instantaneous measurements and modelling, but validation of the results has not been consistently carried out using robust statistical metrics (Junarto, 2021). Previous research (Halulanga et al. 2021) was also conducted at the PLTU PT. X Kendari, but it was limited to direct measurements without using air dispersion modelling or comparing the results of both.

While previous studies have employed the AERMOD model to simulate pollutant dispersion in various industrial contexts, a significant research gap remains regarding the lack of statistical validation using local

ambient data, particularly in Southeast Sulawesi. Most existing studies in similar regions focus solely on simulation results without comparing them to direct field measurements through rigorous statistical testing. The novelty of this research lies in its integrated approach that performs preliminary performance evaluation using local ambient air data collected directly from the PLTU PT.X vicinity by applying multi-parameter statistical indicators, including Root Mean Square Error (RMSE), Mean Bias Error (MBE), and Correlation Coefficient (R), this study seeks to assess the level of agreement between the model and short-term field observations. Furthermore, this study provides an initial dispersion profile for PLTU PT.X, addressing the absence of prior research in this specific power plant. Therefore, this study aims to analyze SO₂ and NO₂ concentrations around the PLTU PT.X through direct measurements, model their dispersion patterns using AERMOD, and evaluate the model's performance during representative operational periods, while acknowledging the temporal constraints of the field data.

2. MATERIALS AND METHODS

2.1. Study area

This study was conducted around the PLTU PT.X in Lalonggasumeeto Subdistrict, Konawe Regency, Southeast Sulawesi, Indonesia, with two ambient air monitoring points (Point 1 in the area of PLTU PT.X and Point 2 in Nii Tanasa Village). The location of monitoring points was determined in accordance with SNI 19-71196-2005 to ensure representation of the potential impact zone from the pollutant. The selection of these two points was strategically based on the prevailing wind direction and the proximity to sensitive receptors; Point 1 represents the area of maximum potential concentration near the emission source, while Point 2 represents the nearest residential area located downwind. This placement ensures that even with a limited number of points, the study captures the most critical spatial variability of pollutant impact on both the industrial site and the surrounding community. The research location map is shown in Figure 1.

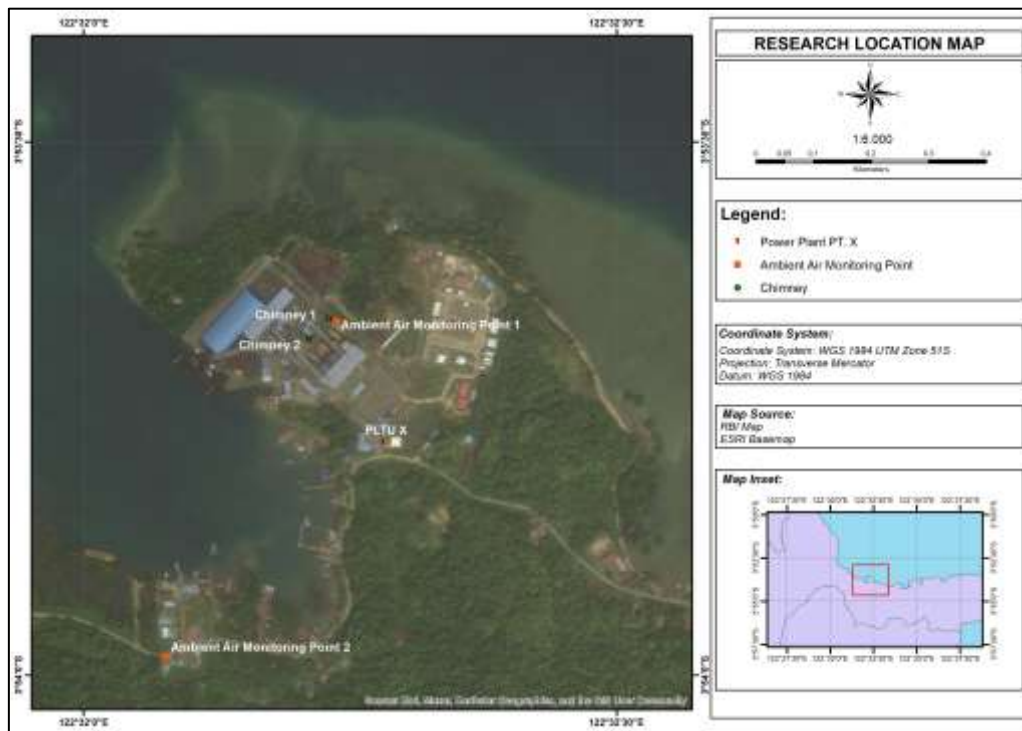


Fig 1: Research location map

2.2. Data collection

Data collection consists of primary and secondary data. Primary data include direct measurements of SO_2 and NO_2 concentrations at two specified points, which are then evaluated against the Indonesian Ambient Air Quality Standards (Government Regulation Number 22 of 2021). Secondary data include meteorological data and chimney specifications of PLTU PT. X and topographic maps, which serve as important input data for dispersion modelling using AERMOD software. The model's performance was evaluated by comparing AERMOD predictions with direct measurement data corresponding to the specific sampling periods using Root Mean Square Error (RMSE), Mean Bias Error (MBE), and Correlation Coefficient (R).

2.2.1. Ambient air sampling

Ambient air sampling for SO_2 and NO_2 was carried out using an Impinger Air Sampler, as shown in Figure 2 below.

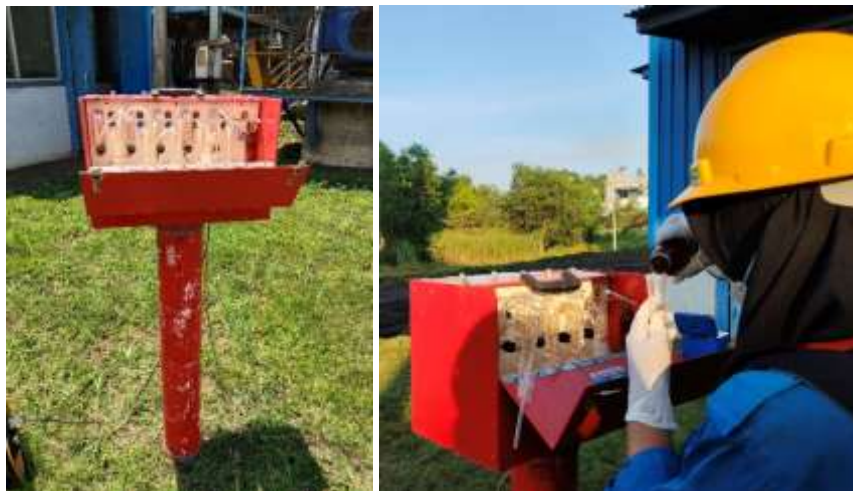


Fig 2: Impinger air sampler

Field measurements were conducted on October 21, 2024, which represents the transition period between the dry and rainy seasons in Southeast Sulawesi. To capture diurnal atmospheric variations, sampling was performed at four specific time intervals: morning (07:00–08:00 WITA), afternoon (13:00–14:00 WITA), evening (16:00–17:00 WITA), and night (19:00–20:00 WITA). These discrete measurements were utilized as preliminary diurnal representative spot samples to evaluate the level of agreement between field observations and the AERMOD model's hourly performance. While this one-day sampling does not constitute a continuous 24-hour integrated average, the sampling intervals followed the representative time-frequency guidelines outlined in the Regulation of the Minister of Environment and Forestry of the Republic of Indonesia Number 27 of 2021 concerning Guidelines for Ambient Air Quality Monitoring. To account for long-term variability, the AERMOD simulation itself utilized a comprehensive one-year hourly meteorological dataset for 2024. This approach allows for a comparison between predicted and observed concentrations during specific atmospheric windows, although it is acknowledged that a more extensive monitoring dataset would be required for a full-scale seasonal or annual model validation.

2.2.2. Meteorological data

Meteorological data for 2024, including cloud cover, temperature, humidity, air pressure, wind direction, wind speed, ceiling height, precipitation, and solar radiation, were obtained from the Copernicus website, while station information was obtained from the Kendari Maritime Meteorological Station (BMKG). This data was processed using WRPLOT, which visualises dominant wind patterns. The complete dataset was then processed using AERMET to generate input files for AERMOD to determine the direction of pollutant dispersion in the atmosphere. The Copernicus dataset was utilized because it provides continuous, high-resolution hourly atmospheric parameters including solar radiation and cloud cover which are essential for the AERMET processor and often unavailable at single surface stations. To ensure local representativeness, this data was synchronized with the coordinates and surface characteristics of the Kendari Maritime Meteorological Station, ensuring the modeled meteorological profile aligns with the specific geographic and climatic conditions of the study area. Details of the meteorological stations information are listed in Table 1.

Table 1: Meteorological station information

Information Type	Description
Station Name	Kendari Maritime Meteorological Station
Station ID	97144
Latitude	03° 58' 12.360" S
Longitude	122° 35' 22.200" E
City	Kendari
State	Indonesia
Station Elevation	2 m
Time Zone	WITA (UTC +8)

2.2.3. PLTU PT.X chimney specifications

The technical specifications of the chimneys, including height, diameter, gas exit velocity, and temperature, were obtained from the PLTU PT.X operational reports for February 2024, as presented in Table 2. These physical parameters are essential for determining the plume rise and initial dispersion behavior in the AERMOD model. To ensure the accuracy of the emission input, the emission rates (g/s) were calculated using the U.S. EPA emission factor method based on fuel consumption, while the measured stack concentrations from the Analysis Report were utilized to verify and ensure that the calculated rates were consistent with the actual monitored conditions.

Table 2: Chimney physical specifications of PLTU PT.X

No.	Parameters	Chimney 1	Chimney 2
1	Chimney Coordinate (UTM) X	448618.00	448585.00
	Chimney Coordinate (UTM) Y	9569519.00	9569480.00
2	Fuel Type	Lignite Coal	Lignite Coal
3	Chimney Height (m)	45	45
4	Chimney Diameter (m)	2.2	2.2
5	Gas Temperature (°C)	129	130
6	Gas Exit Velocity (m/s)	4.72	4.83
7	Emission Flow Rate (m ³ /s)	17.9	18.31
8	Fuel Consumption (tons/month)	9000	9000
9	Elevation (m)	10	10

2.3. Data analysis

Data analysis was performed using measured ambient air concentration data and secondary input data (meteorological and emission data). The analysis procedures performed in this study included:

2.3.1. Processing meteorological data with WRPLOT

The WRPLOT is used to process meteorological data into Windrose maps, which visually depict the direction and speed of prevailing winds during the study period. The results are saved in SAMSON (.SAM)

format for use as input to the AERMET processor. The stages of data processing in WRPLOT are shown in Figure 3.



Fig 3: WRPLOT data processing stages

The Windrose map generated is meteorological input data for dispersion model simulations in AERMOD. The dominant wind direction and speed patterns greatly determine the potential spread of pollutants. The 2024 Windrose map is presented in Figure 4 below.

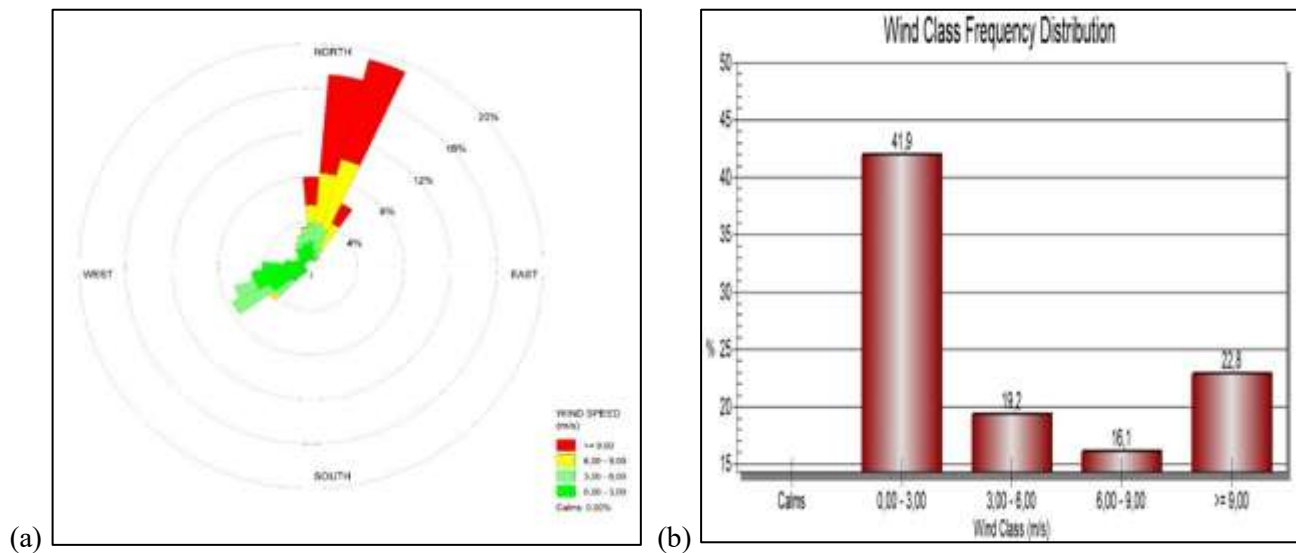


Fig 4: (a) Windrose Map 2024. (b) Wind Class Frequency Distribution

Based on Figures 4a and 4b, the results of the 2024 windrose map analysis show that the dominant direction for the highest wind speed (>9.00 m/s) is North, with a frequency of 22.8%. The most frequent wind class is the low speed range (0.00-3.00 m/s), which blows mainly from the West and contributes the highest frequency of 41.9%. This dominant wind pattern is crucial for understanding the potential spread of pollutants originating from steam power plant.

2.3.2. Calculation of Emission Rate

To meet the input requirements of the AERMOD dispersion model, the emission rates were determined in grams per second (g/s). The calculation of the flue gas emission rate was carried out to estimate the stack emissions based on February 2024 operational data and to calculate the emission values for October 2024 using the United States Environmental Protection Agency (U.S. EPA, 2024) emission factor method (Equation 1). Instead of relying solely on concentration-to-mass conversion, this study utilized an activity-based approach where monthly fuel consumption data were converted into a continuous mass flow rate (tons/second). This ensures

that the resulting emission values reflect the plant's actual operational load during the study period. The calculation results, incorporating the efficiency of the emission control systems, are listed in Table 3.

$$E = A \times EF \times [1 - (ER/100)] \quad \dots(1)$$

where: E – gas emission rate (g/s), A – amount of fuel burned (converted from tons/month to tons/second), EF – emission factor (lb/ton or g/ton), ER – emission control efficiency (if there is a scrubber or other system) (e.g. 0.90 for 90%).

The mass emission rates (E) used as AERMOD inputs were derived through a clear, step-by-step application of the activity-based approach. First, the monthly fuel consumption of 9000 tons was converted into a continuous mass flow rate (A) by dividing it by the total seconds in a 30-day month, resulting in 0.00347 tons/second. This value was then applied to Equation 1 using the U.S. EPA emission factors (EF) of 15.15 kg/ton for SO₂ and 3.86 kg/ton for NO₂, while incorporating the efficiency of the emission control systems (ER) of 90% and 85%, respectively. This calculation process yielded final emission rates of 5.26 g/s for SO₂ and 2.01 g/s for NO₂ per chimney. These derived rates serve as the definitive source-term inputs for the dispersion model, ensuring the simulation reflects the plant's actual operational load during the study period. The complete results of this emission rate calculation are listed in Table 3.

Table 3: Emissions rate calculation results

Parameters	SO ₂		NO ₂	
Emission Factor (lb/ton)	33.4		8.5	
Emission Factor (kg/ton)	15.15		3.86	
Fuel Consumption (tons/month)	9000		9000	
Fuel Consumption (tons/second)	0.00347		0.00347	
Emission Control Efficiency (%)	90		85	
Emission Rate (g/s)	C1	C2	C1	C2
	5.26	5.26	2.01	2.01

Notes: C1 (chimney 1); C2 (chimney 2)

2.3.3. AERMET processing

AERMET processes hourly meteorological data (in .SAM format) and upper-air data to prepare input files for AERMOD. This processing includes calculating surface parameters (such as albedo, bowen ratio, and surface roughness) based on land-use characteristics. In this study, the surface parameters were determined based on the site-specific land-use characteristics surrounding PLTU PT.X. The values assigned for the AERMET processing were an Albedo of 0.13, a Bowen Ratio of 0.47, and a Surface Roughness Length of 0.22 meters. These parameters, combined with hourly meteorological data and upper-air profiles derived from the Copernicus ERA5 dataset, allow AERMET to internally calculate the atmospheric mixing height and the stability of the air layers. AERMET outputs are surface meteorological files (.SFC) and profile files (.PFC) that are ready for use in AERMOD dispersion modelling. Figure 5 illustrates the processing steps for AERMET.

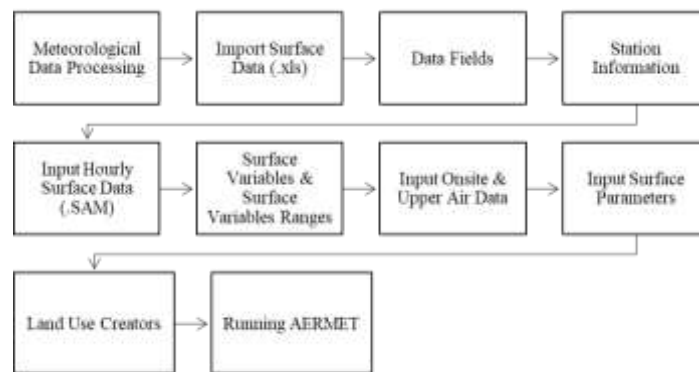


Fig 5: AERMET processing stages

2.3.4. AERMOD processing

Model settings include Control Pathway (defining SO₂ and NO₂ pollutants with an average time of 1 hour), Source Pathway (using stack data and emission rates), Receptor Pathway (Cartesian grid for concentration analysis), and Meteorology Pathway (.SFC and .PFL format files from AERMET). AERMAP is used to integrate topographic data (SRTM3 elevation) into the model grid. Once the data is complete, AERMOD is run for dispersion simulation, producing visualisations of pollutant concentration distributions in the form of maps and isoconcentration lines. Dispersion model processing using AERMOD follows the steps in Figure 6 below.

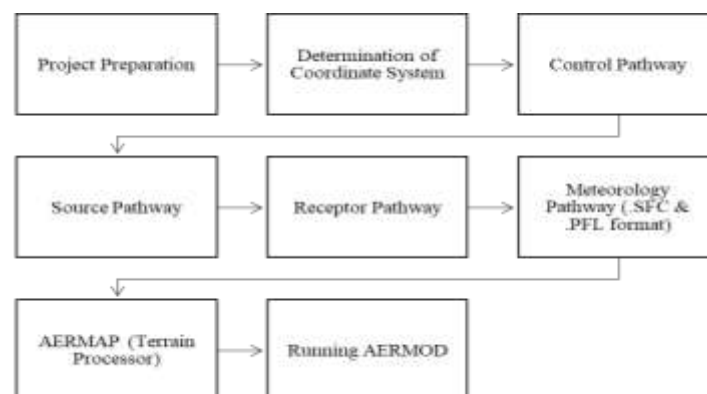


Fig 6: AERMOD processing stages

2.3.5. Model validation test

The model's performance was evaluated by comparing the SO₂ and NO₂ concentrations from short-term ambient air field measurements with the corresponding AERMOD-simulated values. The statistical methods employed for this performance assessment include the calculation of Root Mean Square Error (RMSE), Mean Bias Error (MBE), and Correlation Coefficient (R). These indicators serve to measure the level of agreement between the model's predictions and the observed data during the specific sampling intervals. The RMSE calculation (Hodson, 2022) can be performed using Equation 2.

$$\text{RMSE} = \sqrt{\frac{1}{n} \sum_{i=1}^n (Y_i - \hat{Y}_i)^2} \quad \dots(2)$$

where: RMSE – Root Mean Square Error, Y_i – actual concentration value, \hat{Y}_i – simulated concentration value, n – total number of measurement points.

The Mean Bias Error (MBE) calculation can be performed using Equation 3.

$$MBE = \frac{1}{n} \sum_{i=1}^n (\hat{Y}_i - Y_i) \quad \dots(3)$$

where: MBE – Mean Bias Error, \hat{Y}_i – simulated concentration value, Y_i – actual concentration value, n – total number of measurement points.

The Correlation Coefficient (R) calculation can be performed using Equation 4.

$$R = \frac{\sum_{i=1}^n (\hat{Y}_i - \bar{\hat{Y}})(Y_i - \bar{Y})}{\sqrt{\sum_{i=1}^n (\hat{Y}_i - \bar{\hat{Y}})^2 \sum_{i=1}^n (Y_i - \bar{Y})^2}} \quad \dots(4)$$

where: R – Correlation Coefficient, \hat{Y}_i – simulated concentration value, $\bar{\hat{Y}}$ – mean of simulated concentrations, Y_i – actual concentration value, \bar{Y} – mean of observed concentrations, n – total number of measurement points.

3. RESULTS AND DISCUSSION

3.1. Direct measurement of SO₂ and NO₂ concentrations

Figure 7 below shows a graph of direct measurements of SO₂ and NO₂ concentrations during a 1-hour observation period at two monitoring locations, the PLTU PT. X area and Nii Tanasa Village, based on the intervals of morning, afternoon, evening, and night.

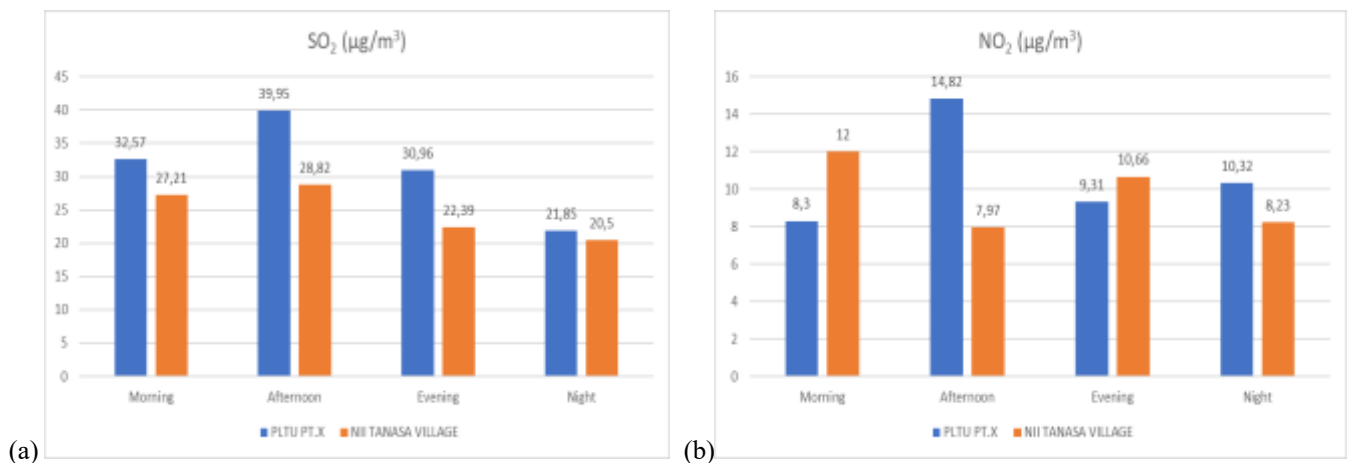


Fig 7: (a) SO₂ direct measurement. (b) NO₂ direct measurement

Based on the graph, for SO₂ (Figure 7a), the highest concentrations at both points occurred during the day (PLTU PT.X monitoring point = 39.95 µg/m³; Nii Tanasa Village monitoring point = 28.82 µg/m³). This trend shows that peak operational activity at the coal-fired power plant significantly increases SO₂ emissions during the day. Lower concentrations were observed at the Nii Tanasa Village monitoring point (approximately 700 m away) compared to the monitoring point near PLTU PT. X, mainly due to the distribution and distance from the emission source, as well as the influence of meteorological factors. In addition, this may be due to weather

factors such as air humidity, wind direction, and temperature, which affect gas dispersion, resulting in SO₂ concentrations at the Nii Tanasa Village location remaining below the quality standard (Halulanga, 2021).

Similar conditions were also observed for NO₂ concentrations (Figure 7b), with the highest value at the PLTU PT.X monitoring point occurring during the day (14.82 µg/m³) due to increased power plant activity. These high concentrations coincided with the highest measured air temperature (34.3 °C) and the lowest humidity (41%) during the day, making the pollutants more stable in the atmosphere. In contrast, at the Nii Tanasa Village monitoring point, the highest concentration was observed in the morning at 12 µg/m³. This suggests that the difference in concentration between the two monitoring points confirms the strong influence of distance from the emission source, although local factors such as morning traffic may also contribute. However, the highest concentrations measured during 1 hour for SO₂ (39.95 µg/m³) and NO₂ (14.82 µg/m³) at both monitoring locations were still below the ambient air quality standards for 1 hour set by Government Regulation Number 22 of 2021 (SO₂ limit: 150 µg/m³; NO₂ limit: 200 µg/m³).

3.2. AERMOD SO₂ and NO₂ concentrations

3.2.1. SO₂ Concentration

Table 4 presents the AERMOD one-hour SO₂ concentrations across four time intervals synchronized with the direct measurement periods, showing that the overall highest concentrations occurred at the PLTU PT.X monitoring point, with a peak value of 31.87 µg/m³ recorded at night. The high concentration at this point correlates with its closer proximity to the primary emission source compared to Nii Tanasa Village. Furthermore, based on the wind rose (Figure 4), although dominant wind directions vary, SO₂ is a local pollutant whose concentrations tend to be highest at locations nearest to the emission source. The phenomenon of increased nighttime concentrations, particularly at the PLTU PT.X monitoring point, indicates the influence of stable atmospheric conditions. According to Kusumawati (2025), atmospheric stability is significantly higher at night than during the day. Variations in atmospheric stability levels can occur based on the intensity of temperature differences between the air mass and the surrounding air (Sasmita et al. 2021). The cooling air at the PLTU PT.X monitoring point during the night is further evidenced by monitoring data, which showed a temperature of 26.5°C and high humidity of 76.7%. Conversely, in Nii Tanasa Village, the peak concentration of 10.81 µg/m³ occurred in the morning. This is likely due to the prevailing stable temperature and humidity conditions; at 29.9°C and 62.3% humidity, the SO₂ concentrations modeled by AERMOD remained insufficiently dispersed into the higher atmospheric layers. Stable atmospheric conditions in the morning restrict vertical air movement, causing pollutants to be trapped near the ground surface (the accumulation phase) before rising daytime temperatures trigger vertical dilution.

Table 4: AERMOD SO₂ concentration

Monitoring Point	Coordinate Point		Time	SO ₂ Concentration (µg/m ³)
	UTM X	UTM Y		
PLTU PT.X	448623,28	9569522,39	Morning	30.92
			Afternoon	22.84
			Evening	20.23
			Night	31.87
Nii Tanasa Village	448364,13	9568947,04	Morning	10.81
			Afternoon	8.41
			Evening	8.41
			Night	7.23

3.2.2. NO₂ Concentration

Table 5 presents the AERMOD one-hour NO₂ concentrations across four time intervals (morning, afternoon, evening, and night) synchronized with the direct measurement periods. At the PLTU PT.X monitoring point, the highest NO₂ concentration significantly occurred at night, reaching 10.56 µg/m³, which is higher than the concentrations recorded during the morning, afternoon, and evening at the same location. A similar pattern of significant nighttime increase was observed in Nii Tanasa Village, with a concentration of 4.45 µg/m³. The increase in NO₂ concentrations at night in these two locations also indicates stable atmospheric conditions, such as temperature inversions, which trap air movement. Similar to SO₂ concentrations, AERMOD measures temperature and humidity at night, which are more stable. This inhibits vertical air movement and affects pollutants near the ground surface, leading to increased pollution at the human respiratory level (Srisantyorini, 2025).

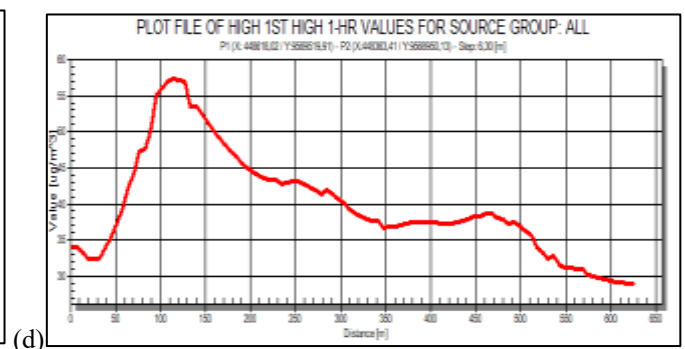
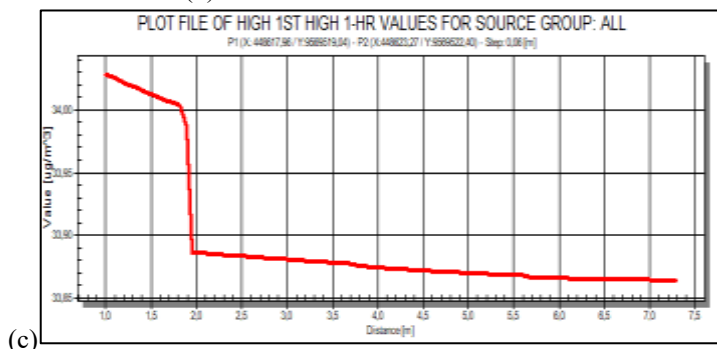
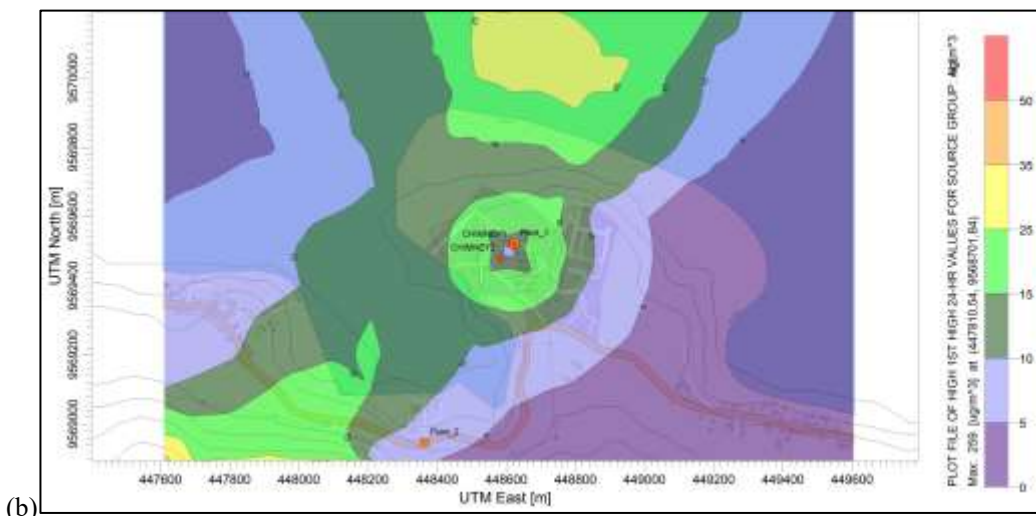
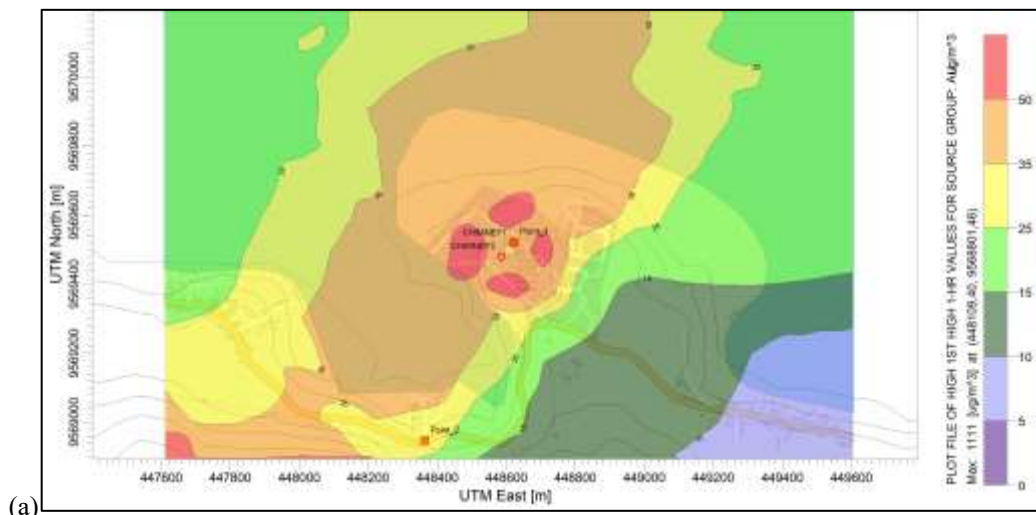
Table 5: AERMOD NO₂ concentration

Monitoring Point	Coordinate Point		Time	NO ₂ Concentration (µg/m ³)
	UTM X	UTM Y		
PLTU PT.X	448623,28	9569522,39	Morning	7.87
			Afternoon	7.37
			Evening	7.37
			Night	10.56
Nii Tanasa Village	448364,13	9568947,04	Morning	3.33
			Afternoon	3.06
			Evening	3.06
			Night	4.45

3.3. AERMOD dispersion modeling

3.3.1. Dispersion of SO₂

After dispersion for 1 hour and 24 hours, Figures 8 (a) and (b) show that the maximum concentrations for the highest average 1-hour SO₂ concentrations at the monitoring points of PLTU PT.X and Nii Tanasa Village were 33.86 µg/m³ and 29.05 µg/m³, respectively. At the same time, the highest 24-hour averages were 10.65 µg/m³ and 7.42 µg/m³. Meanwhile, Figures 8 (c), (d), (e), and (f) illustrate the relationship between concentration and distance during that period based on the prevailing wind direction.



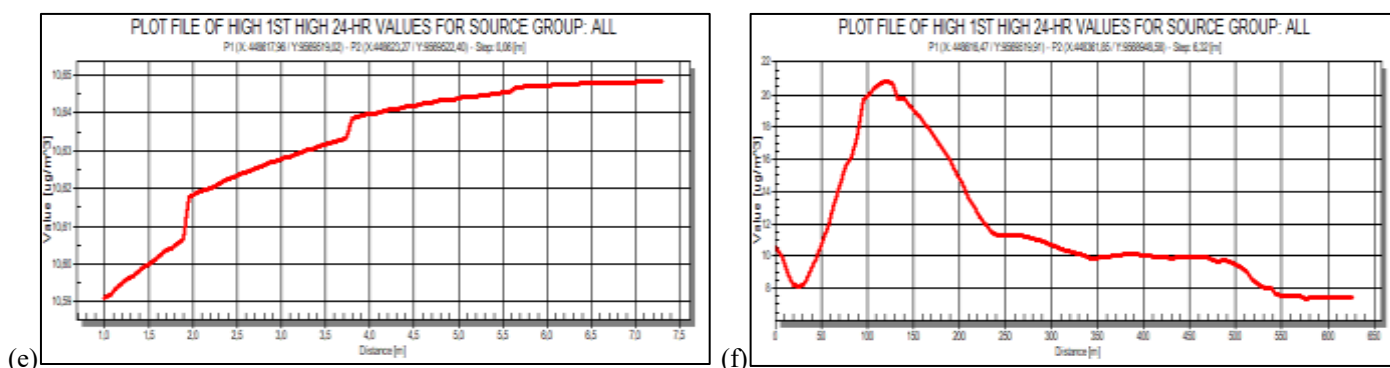
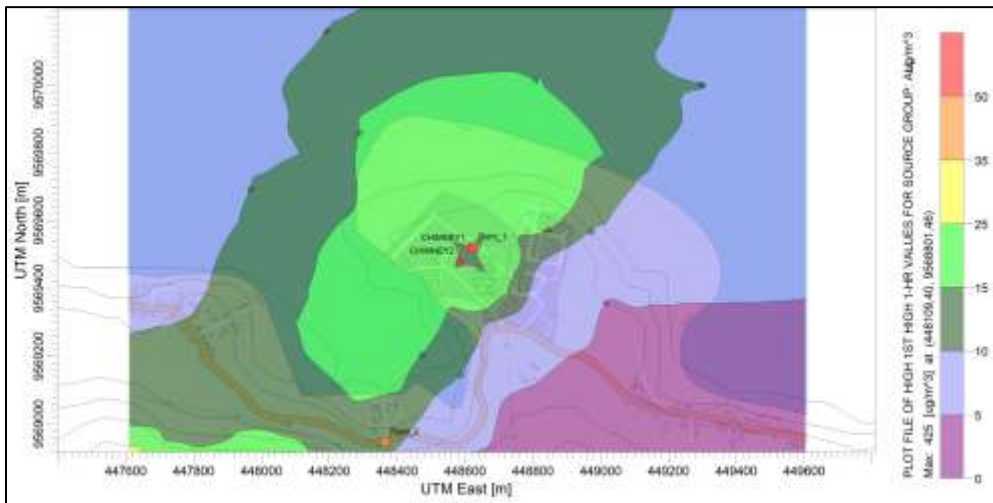


Fig 8: (a) 1-hour SO₂ dispersion. (b) 24-hour SO₂ dispersion. (c) SO₂ at point 1 (PLTU PT.X) 1 hour. (d) SO₂ at point 2 (Nii Tanasa Village) 1 hour. (e) SO₂ at point 1 (PLTU PT.X) 24 hours hour. (f) SO₂ at point 2 (Nii Tanasa Village) 24 hours.

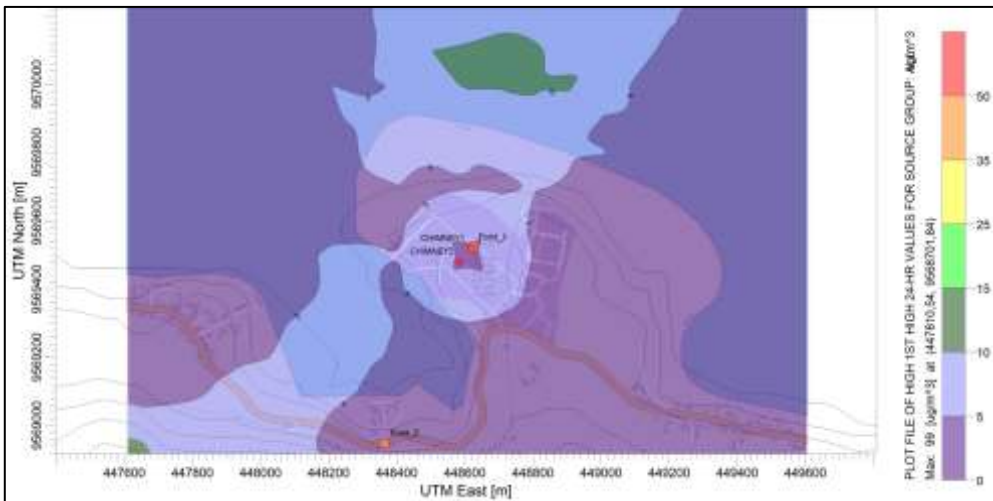
The SO₂ distribution pattern during the 2024 period predominantly points north-northeast toward the sea, following the prevailing wind direction. At the PLTU PT.X monitoring point (± 7.5 meters from the stack base), Figure 8(c) shows initial predicted concentrations of approximately 34.02 $\mu\text{g}/\text{m}^3$. However, it should be noted that for a 45 meter stack, receptors located within this immediate near-field zone (1–7.5 meters) fall below the typical plume trajectory. While the model accounts for building downwash effects where aerodynamic turbulence can influence dispersion the physical meaningfulness of predictions at such close proximity is limited, as the plume has not yet fully reached ground level. In contrast, a more dynamic and physically representative pattern is observed towards Nii Tanasa Village (Figure 8(d)). This area shows a classic dispersion profile where the concentration reached a significant peak of approximately 57 $\mu\text{g}/\text{m}^3$ at a distance of 110–120 meters from the source, representing the primary plume touchdown point. After this peak, the concentration gradually decreased and stabilized, reaching 29.05 $\mu\text{g}/\text{m}^3$ at the monitoring point in Nii Tanasa Village (± 650 meters). For the 24-hour average (Figure 8(e) and 8(f)), the maximum concentrations at the PLTU PT.X and Nii Tanasa Village receptors were 10.65 $\mu\text{g}/\text{m}^3$ and 7.42 $\mu\text{g}/\text{m}^3$, respectively. All predicted values remained well below the ambient air quality standards (150 $\mu\text{g}/\text{m}^3$ for 1-hour and 75 $\mu\text{g}/\text{m}^3$ for 24-hour). These findings are consistent with Sarwono et al. (2022), noting that concentration patterns are heavily influenced by dominant wind directions and distance-dependent dispersion factors.

3.3.2. Dispersion of NO₂

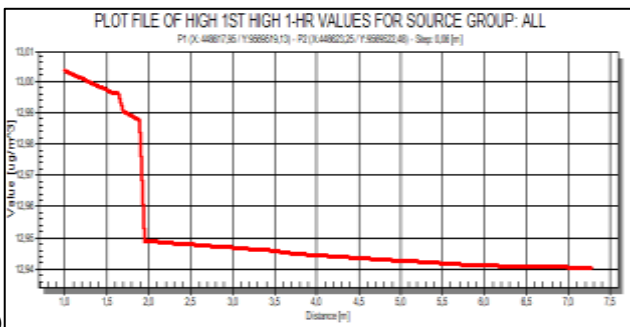
As with SO₂, for NO₂ concentrations after dispersion for 1 hour and 24 hours, Figures 9 (a) and (b) show the maximum concentration values for the highest 1-hour average at the PLTU PT.X and Nii Tanasa Village monitoring points, which were 12.94 $\mu\text{g}/\text{m}^3$ and 11.10 $\mu\text{g}/\text{m}^3$, respectively. At the same time, the highest 24-hour averages were 4.07 $\mu\text{g}/\text{m}^3$ and 2.83 $\mu\text{g}/\text{m}^3$. Meanwhile, Figures 8 (c), (d), (e), and (f) illustrate the relationship between concentration and distance during that period based on the prevailing wind direction.



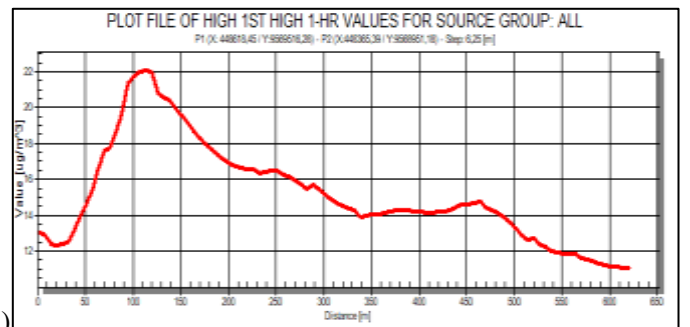
(a)



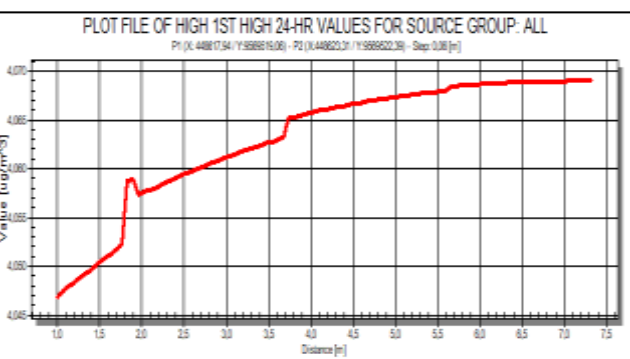
(b)



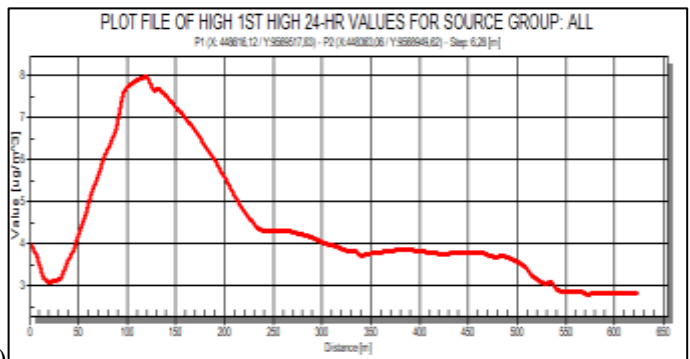
(c)



(d)



(e)



(f)

Fig 9: (a) 1-hour NO₂ dispersion. (b) 24-hour NO₂ dispersion. (c) NO₂ at point 1 (PLTU PT.X) 1 hour. (d) NO₂ at point 2 (Nii Tanasa Village) 1 hour. (e) NO₂ at point 1 (PLTU PT.X) 24 hours hour. (f) NO₂ at point 2 (Nii Tanasa Village) 24 hours

The NO₂ dispersion pattern during the 2024 period follows a similar trend to SO₂, predominantly spreading north-northeast from the PLTU PT.X chimney toward the sea, reflecting the influence of the prevailing wind direction. Figure 9(c) illustrates the NO₂ concentration within the immediate near-field zone (up to 7.5 meters) from the stack base. While the model calculates an elevated concentration of 12.94 µg/m³ at this point, it is acknowledged that for a 45 meter stack, receptors at this distance are situated below the primary plume trajectory. These near-field values should be interpreted with caution, as they may reflect the model's mathematical treatment of aerodynamic turbulence (building downwash) rather than a physically representative grounding of the plume so close to the source. Meanwhile, for the 24-hour average (Figure 9(e)), the dispersion follows a smaller scale with a maximum concentration of 4.07 µg/m³ at the same receptor.

In contrast, the dispersion toward Nii Tanasa Village (Figure 9(d)) shows a more physically representative and classic dispersion pattern. The concentration exhibits an upward trend, peaking at approximately 22 µg/m³ at a distance of 100 meters from the source. This peak represents the plume touchdown point, occurring after the plume undergoes thermal buoyancy (plume rise) and reaches the ground-level due to wind transport, before gradually decreasing to 11.10 µg/m³ at the ±650 meters receptor. A similar trend is observed for the 24-hour average (Figure 9(f)), which peaks at 8 µg/m³ within the 100–150 meter range before declining to 2.83 µg/m³ at the monitoring point. Despite these fluctuations, all NO₂ concentration values remained well below the national ambient air quality standards (200 µg/m³ for 1-hour and 65 µg/m³ for 24-hour).

3.4. Model validation test (RMSE, MBE, & R)

Table 6 presents a comparison between the SO₂ and NO₂ concentrations obtained from direct measurements and the AERMOD model predictions at two monitoring points: the PLTU PT.X and Nii Tanasa Village. To ensure a valid comparison, the AERMOD model output selected for this analysis was synchronized with the exact date and hourly intervals (morning, afternoon, evening, and night) of the field sampling conducted on October 21, 2024. While this temporal alignment allows for a snapshot performance check, it is acknowledged that a single day of data is insufficient to fully represent the model's annual simulation. Direct monitoring results show that SO₂ concentrations near the PLTU PT.X ranged from 21.85 µg/m³ to 39.95 µg/m³, while AERMOD estimated 20.23 µg/m³ to 31.87 µg/m³. These discrepancies are primarily due to the receptor's close proximity to the emission source (±7.5 meters). For a 45 meter stack, this distance falls outside the physically meaningful predictive zone of AERMOD, as the exhaust gas is still in the buoyancy (plume rise) phase and has not yet grounded. Consequently, the higher field measurements at this location likely capture low-level fugitive emissions or local background sources within the plant area that are not accounted for in the stack-only model. A similar pattern was observed for SO₂ parameters, where field measurements ranged from 8.3 µg/m³ to 14.82 µg/m³, while the AERMOD simulation estimated lower concentrations between 7.37 µg/m³ and 10.56 µg/m³ due to the same near-field modeling limitations.

Meanwhile, at the Nii Tanasa Village monitoring point (± 650 meters), the AERMOD model showed a better alignment with the dispersion physics, although simulated values were still lower than direct measurements. For SO_2 , field measurements ranged from $20.5 \mu\text{g}/\text{m}^3$ to $28.82 \mu\text{g}/\text{m}^3$, whereas AERMOD estimated $7.23 \mu\text{g}/\text{m}^3$ to $10.81 \mu\text{g}/\text{m}^3$. Similarly, for NO_2 , field measurements ranged from $8.23 \mu\text{g}/\text{m}^3$ to $12 \mu\text{g}/\text{m}^3$, while AERMOD modeling results ranged from $3.06 \mu\text{g}/\text{m}^3$ to $4.45 \mu\text{g}/\text{m}^3$. These results indicate that AERMOD is more representative at greater distances where the plume has undergone diffusion and wind transport. Consistent with Ramdhani (2017), discrepancies may arise because field monitoring captures cumulative impacts from various sources, such as traffic and community activities, while the model focuses strictly on boiler stack emissions. Therefore, given the inherent modeling uncertainties and the limited sampling duration, these results should be interpreted as a preliminary screening-level assessment.

Table 6: Comparison of direct measurements with the AERMOD model

Monitoring Point	Parameters	Time	Direct Measurement	AERMOD
PLTU PT.X	SO_2 ($\mu\text{g}/\text{m}^3$)	Morning	32.57	30.92
		Afternoon	39.95	22.84
		Evening	30.96	20.23
		Night	21.85	31.87
	NO_2 ($\mu\text{g}/\text{m}^3$)	Morning	8.3	7.87
		Afternoon	14.82	7.37
		Evening	9.31	7.37
		Night	10.32	10.56
Nii Tanasa Village	SO_2 ($\mu\text{g}/\text{m}^3$)	Morning	27.21	10.81
		Afternoon	28.82	8.41
		Evening	22.39	8.41
		Night	20.5	7.23
	NO_2 ($\mu\text{g}/\text{m}^3$)	Morning	12	3.33
		Afternoon	7.97	3.06
		Evening	10.66	3.06
		Night	8.23	4.45

To evaluate the performance of the AERMOD model in predicting the concentrations of SO_2 and NO_2 , statistical performance assessment was performed by comparing the model results with direct field measurements. Table 7 presents the results of the Root Mean Square Error (RMSE) calculated based on Equation 2, Mean Bias Error (MBE) calculated based on Equation 3, and Correlation Coefficient (R) calculated based on Equation 4 with calculated using 8 paired datasets for each pollutant.

The validation results show that the RMSE values for SO_2 and NO_2 are $14.00 \mu\text{g}/\text{m}^3$ and $5.37 \mu\text{g}/\text{m}^3$, respectively. These values indicate that the average deviation between the model predictions and actual

measurements is relatively small when compared to the national ambient air quality standards. Since RMSE represents the standard deviation of the residuals, these results suggest that the model's predictions deviate within a reasonable range from the actual field measurements. The low RMSE values, when compared to the observed mean, suggest that the AERMOD model is capable of predicting concentration magnitudes within a comparable range to the observed values at the study site. This is consistent with the principle that a smaller RMSE (approaching 0) signifies a better fit between the modeled and measured data, providing an initial indication of the model's performance for further spatial analysis (Hamdanah & Fitriana, 2021). Thus, the model's error magnitude remains within an acceptable range for a screening-level assessment, suggesting that the predicted concentrations show a reasonable agreement with the actual field variations in terms of absolute magnitude within the sampled periods.

The Mean Bias Error (MBE) was employed to assess the systematic bias of the forecasting model by measuring the average difference between the predicted and actual values (Kato, 2016). The calculation yielded negative MBE values for both pollutants: $-10.44 \mu\text{g}/\text{m}^3$ for SO_2 and $-4.32 \mu\text{g}/\text{m}^3$ for NO_2 . According to Kato (2016), a negative MBE indicates that the forecasted values are, on average, smaller than the actual values, signifying a systematic underprediction. In the context of this study, this trend is commonly observed in dispersion modeling when the simulation focuses primarily on specific point sources, such as the power plant stack, while actual field measurements capture the cumulative impact of additional background concentrations from other local activities or non-modeled sources. Despite this slight underprediction, the scores remain relatively close to the ideal value of 0.0, and the resulting concentrations remain consistently below national regulatory thresholds, supporting the potential use of the model for preliminary environmental impact screening.

Regarding the Correlation Coefficient (R), the model yielded values of 0.36 for SO_2 and 0.12 for NO_2 . According to Thieu et al. (2023), the correlation coefficient quantifies the strength and direction of the linear relationship between two variables, where a best possible score is 1.0 and a value close to 0 indicates no correlation. These results indicate a weak linear relationship for SO_2 and a negligible correlation for NO_2 , suggesting that the model struggles to capture the precise hourly fluctuations of the pollutants during the sampling period, such results are frequently expected when dealing with a limited number of paired observations ($n=8$) and short-term (1-hour) sampling durations. Furthermore, it is clearly acknowledged that this one-day dataset is limited for validating an AERMOD simulation driven by a full-year meteorological dataset. However, as noted by Thieu et al. (2023), R is commonly used in engineering to study relationships, and when integrated with the low RMSE and MBE results, the AERMOD model demonstrates a useful preliminary performance evaluation for characterizing spatial dispersion patterns during the sampling period in the vicinity of the PLTU PT.X and Nii Tanasa Village, serving as a screening-level assessment rather than a fully validated annual model.

Table 7: RMSE, MBE, & R test results

Parameters	RMSE	MBE	R
SO_2 ($\mu\text{g}/\text{m}^3$)	14	-10.44	0.36
NO_2 ($\mu\text{g}/\text{m}^3$)	5.37	-4.32	0.12

4. CONCLUSIONS

This study concludes that while direct measurements and AERMOD simulations show differing peak intervals (daytime and nighttime, respectively), the resulting pollutant concentrations consistently remain below national ambient air quality standards. The elevated nighttime predictions in AERMOD highlight the influence of stable atmospheric conditions, particularly in the vicinity of the source where the model accounts for building downwash effects, though near-field predictions should be interpreted with caution given the stack height. Spatially, the dispersion follows a north-northeast pattern, with concentrations decreasing significantly as distance increases, indicating that the area closest to the stack receives the highest impact, though still within regulatory limits. Although discrepancies exist between measured and modeled peaks, the AERMOD model demonstrates a useful preliminary performance for characterizing spatial dispersion patterns.

This is supported by RMSE values of 14.00 $\mu\text{g}/\text{m}^3$ for SO_2 and 5.37 $\mu\text{g}/\text{m}^3$ for NO_2 , alongside MBE and R results, which suggest the model's potential suitability for initial screening-level assessments. While current findings show that emissions are within safe regulatory limits, they clearly highlight the inherent limitations of short-term monitoring and emphasize the importance of continuous monitoring and long-term sampling to account for temporal variability. These insights provide an initial framework for guiding future environmental management and policy formation in industrial zones.

Author Contributions: This research was a collaborative effort from all authors. **Nur Miftahuljannah** was responsible for the research conceptualization and design, collection and/or assembly of data, data analysis and interpretation, and writing the article—original draft preparation. **Sumarni Hamid Aly** and **Muralia Hustim** contributed equally to the research conceptualization and design, data analysis and interpretation, and provided critical revision of the article. All authors have read and agreed to the published version of the manuscript.

Funding: This research received no external funding.

Institutional Review Board Statement: Not applicable.

Informed Consent Statement: Not applicable.

Acknowledgments: The author would like to thank PLTU PT.X in Lalongasumeeto District, Konawe Regency, Southeast Sulawesi, Indonesia, for granting the author access and permission to conduct research at the location.

Conflicts of Interest: The authors declare no conflicts of interest.

REFERENCES

1. Alchamdani. 2019. Exposure of NO_2 and SO_2 to Health Risks of Public Fuel Station (SPBU) Workers in Kendari City. *Jurnal Kesehatan Lingkungan*, 11(4), pp. 319-330. [<http://dx.doi.org/10.20473/jkl.v11i4.2019.319-330>]
2. Alviani, M., Anggraini, F.J. and Rodhiyah, Z., 2022. Pemodelan $\text{PM}_{2.5}$ pada Musim Kemarau menggunakan Software Graz Largangan Model di Kecamatan Kota Baru Kota Jambi. *Jurnal Teknik Lingkungan UM Kendari*, 2(2), pp. 5-9. [<https://doi.org/10.51454/teluk.v2i2.529>]

3. Barata, L.O.A. 2024. Sistem Perawatan Water Treatment Plant (WTP) PLTU Nii Tanasa 3 x 10 MW. *Piston Jurnal Teknologi*, 9(1), pp. 24-35. [<https://doi.org/10.55679/pistonjt.v9i1.56>]
4. Government Regulation of the Republic of Indonesia Number 22 of 2021. *Implementation of Environmental Protection and Management* (in Indonesian). Jakarta. [https://jdih.kehutan.go.id/new2/home/open_indonesia_file/PP_22_TAHUN_2021_PENYELENGGARAAN_LH_c_menlhk_02222021144819.pdf]
5. Halulanga, A.J., Rosdiana, R. and Adami, A., 2021. Uji Kandungan Gas Sulfur Dioksida (SO₂) pada Udara Ambien Akibat adanya Pembakaran Batubara PLTU Nii Tanasa, Sulawesi Tenggara. *Jurnal Teknik Lingkungan UM Kendari*, 1(2), pp. 5-10. [<https://doi.org/10.51454/teluk.v1i2.503>]
6. Hamdanah, F.H. and Fitriana, D., 2021. Analisis Performansi Algoritma Linear Regression dengan Generalized Linear Model untuk Prediksi Penjualan pada Usaha Mikra, Kecil, dan Menengah. *Jurnal Nasional Pendidikan Teknik Informatika*, 10(1), pp. 23-32. [<https://doi.org/10.23887/janapati.v10i1.31035>]
7. Hodson, T.O. 2022. Root Mean Square Error (RMSE) or Mean Absolute Error (MAE): When to Use Them or Not. *Journal of Geoscientific Model Development Discussions*, 15(14), pp. 5481-5487. [<https://doi.org/10.5194/gmd-15-5481-2022>]
8. Junarto, G.E. 2021. Penerapan Model Aermod untuk Dispersi Emisi Gas Buangan PLTU dan Analisis Risiko Kesehatan Lingkungan (Studi: PLTU Tonasa, Kec. Bungoro, Kabupaten Pangkep). Master's Thesis, Hasanuddin University, Makassar. [https://repository.unhas.ac.id/id/eprint/15398/2/P032171203_tesis_bab%201-2.pdf]
9. Kato, Takeyoshi. 2016. Prediction of Photovoltaic Power Generation Output and Network Operation. *Integration of Distributed Energy Resources in Power Systems*. pp. 77-108. [<https://doi.org/10.1016/B978-0-12-803212-1.00004-0>]
10. Kusumawati, R.D. 2025. Analisis Dispersi Nitrogen Dioksida (NO₂) Udara Ambien di Kawasan Budaya, Kota Yogyakarta menggunakan pemodelan AERMOD. Skripsi, Universitas Islam Indonesia, Yogyakarta. [<https://dspace.uii.ac.id/bitstream/handle/123456789/56033/21513157.pdf?sequence=1&isAllowed=y>]
11. Ningsih, S. 2020. Model Sebaran SO₂ dan NO_x PLTU Jeneponto PT. Bosowa Energi. *Jurnal AKRAB Juara*, 5(2), pp. 231-238. [<https://www.akrabjuara.com/index.php/akrabjuara/article/view/1079/954>]
12. Nugraha, P.S., Setiawan, A. and Yustian, I., 2023. AERMOD Modeling Analysis of CO And NO_x Parameters from Diesel Generator Emission Sources in the Coal Mining Industry. *Sriwijaya Journal of Environment*, 8(2), pp. 92-97. [<http://dx.doi.org/10.22135/sje.2023.8.2.92-97>]
13. Putra, D.Y.P. and Nisa, S.Q.Z., 2023. Uji Model AERMOD terhadap Emisi di PT. X Jawa Timur. *ESEC Proceeding Environmental Science and Engineering Conference*, 4(1), pp. 370-379. [<https://esec.upnvjt.com/index.php/prosiding/article/download/256/182>]
14. Ramadhani, I.S. 2017. Pemantauan Kualitas Udara Ambien dan Pemodelan Gauss Dispersion Gas Nitrogen Dioksida (NO₂) dari Emisi Industri Kayu Lapis di Dusun Kalimati, Tirtomartani, Kalasan, Sleman, D.I Yogyakarta. Skripsi, Islam Indonesia University, Yogyakarta. [<https://dspace.uii.ac.id/handle/123456789/33142>]
15. Regulation of the Minister of Environment and Forestry of the Republic of Indonesia Number 27 of 2021. *Environmental Quality Index* (in Indonesian). Jakarta. [https://jdih.kehutan.go.id/new2/home/open_indonesia_file/2021pmlhk027_menlhk_12312021144624.pdf]

16. Salari, M., Abdolmaleki, M.J., Shahid, E.S. and Akhouni, B., 2026. Dispersion of Particulate Matter Using AERMOD Model and Health Risk Assessment: Case Study Saveh Gypsum Industry. *Iranica Journal of Energy and Environment*. 17(2), pp. 372-381. [<https://doi.org/10.5829/ijee.2026.17.02.12>]
17. Sarwono, E., Wijayanto, E., Huda, H., Harrits, R.F. and Zain, I.F., 2022. Dispersi SO₂ dan NO₂ dari Cerobong Auxiliary Boiler Industri Methanol PT KMI menggunakan Gaussian Plum Model Aermod di Kota Bontang Kalimantan Timur Indonesia, *Jurnal Chemurgy*, 6(2), pp. 109-117. [<http://e-journals.unmul.ac.id/index.php/TK>]
18. Sasmita, A., Andrio, D. and Nopita, R., 2021. Dispersi SO₂ dan NO₂ dari Pembangkit Listrik Tenaga Uap Tembilahan Riau. *Jurnal Ilmiah Teknik Lingkungan*, 13(2), pp. 98-107. [<https://doi.org/10.33005/envirotek.v13i2.162>]
19. Srisantyorini, T. 2025. *Analisis Kualitas Udara dampak terhadap Lingkungan dan Kesehatan*, 1st ed. Mafy Media Literasi Indonesia: Solok, Indonesia. [<https://penerbitmafy.com/wp-content/uploads/2025/12/ANALISIS-KUALITAS-UDARA-Dampak-Terhadap-Lingkungan-dan-Kesehatan.pdf>]
20. Tampa, G.M., Maddusa, S.S. and Pinontoan, O.R., 2020. Analisis Kadar Sulfur Dioksida (SO₂) Udara di Terminal Malalayang Kota Manado Tahun 2019. *Indonesian Journal of Public Health and Community Medicine*, 1(3), pp. 87-92. [<https://doi.org/10.35801/ijphcm.1.3.2020.29116>]
21. Thieu, N.V., Barma, S.D., Lam, T.V., Kisi, O. and Mahesha, A., 2023. Groundwater Level Modeling using Augmented Artificial Ecosystem Optimization. *Journal of Hydrology*, 617, pp. 129034. [<https://doi.org/10.1016/j.jhydrol.2022.129034>]
22. Tran, Q.A., Nguyen, N.H.T., Nguyen, P.Q. and Nguyen, A.M., 2022. Simulation of Thermal Power Plant Source Contribution to Ambient Air Concentration in Cam Pha City, Quang Ninh province using AERMOD dispersion model. *Journal of Mining and Earth Sciences*, 63(3), pp. 35-42. [[https://doi.org/10.46326/JMES.2022.63\(3\).05](https://doi.org/10.46326/JMES.2022.63(3).05)]
23. United States Environmental Protection Agency (US EPA), 2024. Recommended Procedures for Development of Emissions Factors and Use of the WebFIRE Database. Retrieved May 19, 2025, from [https://www.epa.gov/system/files/documents/2024-09/final-webfire-procedures-document_aug-2024.pdf]
24. Wangsa, D., Bachtiar, V.S. and Raharjo, S., 2022. Uji Model AERMOD terhadap Sebaran Particulate Matter 10 µm (PM10) di Sekitar Kawasan PT Semen Padang. *Jurnal Ilmu Lingkungan*, 20(2), pp. 291-301. [<http://doi.org/10.14710/jil.20.2.291-301>]
25. Zakaria, R., Aly, S.H. and Annisa., 2020. Air Dispersion Modelling of Gas Turbine Power Plant Emissions in Makassar by Using AERMOD. In: *Proceedings of the IOP Conference Series: Earth and Environmental Science*, Makassar, Indonesia. [<https://doi.org/10.1088/1755-1315/419/1/012153>]